Wear 394–395 (2018) 228–235

Contents lists available at ScienceDirect

Wear

journal homepage: www.elsevier.com/locate/wear

Antibiocorrosive epoxy-based coatings with low friction and high scratch resistance

Khatuna Barbakadze[a,b,c,1], Witold Brostow[c,*,1], Tea Datashvili[c,1], Nathalie Hnatchuk[c,1], Nodar Lekishvili[a]

[a] Department of Chemistry, Institute of Inorganic-Organic Hybrid Compounds and Non-traditional Materials, Faculty of Exact and Natural Sciences, Ivane Javakhishvili University, 3 Ilia Chavchavadze Ave., 0179 Tbilisi, Georgia
[b] Department of Medical Chemistry, Faculty of Pharmacy, Tbilisi Medical University, 33 Vazha Pshavela Ave., 0186 Tbilisi, Georgia
[c] Laboratory of Advanced Polymers & Optimized Materials (LAPOM), Department of Materials Science and Engineering, University of North Texas, 3940 North Elm Street, Denton TX 76207, USA

ARTICLE INFO

Keywords:
Polymer scratch resistance
Polymer friction
Polymer aging
Water absorption

ABSTRACT

We have created inorganic-organic hybrid composites and antibiocorrosive coatings based on an epoxy modified with silicon-containing polyepoxies and bioactive coordination compounds. The scratch resistance was determined using a conical diamond indenter with linearly increased load. Repetitive scratching along the same groove (sliding wear determination) was also performed. Whether in single or in repetitive scratching, for most hybrids the residual depth is shallower than for the pure epoxy. Dynamic friction was determined on a pin-on-disk tribometer using steel pins. Lower friction is accompanied by higher scratch resistance. Surface morphology seen in scanning electron microscopy (SEM) shows that increasing modifier content causes more ductile behavior with less crack nucleation; no debris formation is observed. The composites were also characterized by differential scanning calorimetry (DSC) and thermogravimetric analysis (TGA). Isothermal aging and water absorption ability (W_{H2O}) of the hybrids were determined. The hybrids are optically transparent, visually homogeneous, with smooth surfaces.

1. Introduction

Friction is a key materials property, studied already by Leonardo da Vinci who formulated certain relationships describing it in 1493 [1]. Friction of metal surfaces can be mitigated by liquid lubricants, but for polymers such lubricants often cause swelling and other approaches have to be developed [2,3].

While in general the ideas of Leonardo da Vinci seem to retain their validity even today, in some cases there is a complicating factor: *friction is affected by corrosion and biocorrosion*, the latter caused by living organisms [3–7].

The effects of pathogenic microorganisms constitute global hazards for humanity and the environment. These microorganisms appear in natural systems and form complicated aggregates on the surfaces of various natural and synthetic polymers—resulting in irreversible deterioration and non-controlled biodegradation. One of the consequences are significant economic losses to industry and serious threats to the cultural heritage (historic monuments, archeological structures, museum exhibits, etc.) as well [6–8]. The total annual losses are in billions of dollars [9].

An important option in mitigation biodegradation is formation of polymer based hybrid materials, taking advantage of the best properties of each component, decreasing or eliminating their drawbacks, and achieving synergic effects. Low scratch and wear resistance and also environmental degradation have hindered many important applications [4] and long term performance of polymeric materials [10–13] and also their potential or capability for self-organization [14]. Thus, it is essential to achieve unchanged physical and mechanical properties (isothermal aging stability, mechanical strength, tribological properties, etc.) in operational conditions. Important here is reduction of the risk of damage caused by biodestructors by providing inhibition of growth of harmful microorganisms on materials surfaces. In turn, this should enable creation of functional coatings, adhesives, membranes, fuel and solar cells, sensors—used in engineering and also in medicine [8,10,11]. Thus, high abrasion resistance constitutes an important focus or perhaps the leitmotiv of this paper.

Some effective bioactive composites have been made based on polyurethanes [15]. A parallel option consists in using epoxy resins as

* Corresponding author.
E-mail addresses: khbar2016@gmail.com (K. Barbakadze), wkbrostow@gmail.com (W. Brostow), hnatnm@gmail.com (N. Hnatchuk), nodar@lekishvili.info (N. Lekishvili).
[1] www.unt.edu/LAPOM/.

http://dx.doi.org/10.1016/j.wear.2017.08.006
Received 11 September 2016; Received in revised form 18 August 2017; Accepted 18 August 2017
Available online 31 August 2017
0043-1648/

matrices—given their good thermal, electrical and adhesive properties [16–18]. However, epoxy-based composites tend to have low strength, low resistance to brittle fracture and propensity for crack formation and growth [19]. Options used earlier involved the use of poly(dimethylsiloxane) particles [19] or else polysiloxane–polycaprolactone block copolymers [20].

The present work is related to some extent to earlier work by some of us [21–23] and also by Travinskaia and her colleagues [24]; more on this below. Now we have directed our work towards development of novel inorganic-organic hybrid materials with low friction, high abrasion resistance, as well as high stability to biocorrosion induced by various microorganisms or fungi. These properties have been achieved by combining different molecular building blocks and verified by determination of the resulting properties.

2. Experimental

2.1. Materials

The basic matrix component for antibiocorrosive coatings was a commercial epoxy called ED-20, made in the Institute of Polymeric Materials in Sumgaiyt, Azerbaijan, by reaction of one mole of bisphenol A with two moles of epichlorohydrin (epoxy number = 20; viscosity = 5–15 Pa s.). Silicon-organic diepoxy with functional $-CH_2Cl$ groups at silicon atoms (molar mass determined by ebulliometry $M_{ebul} \approx 386$); 21.7% epoxy groups, see Scheme 1a; and α,ω-dihydroxydimethyl(methylvinyl)oligoorganosiloxane (η = 2.7 Pa.s, $M_{ebul} \approx 2.95.10^4$; see Scheme 1c) were synthesized and provided to us by Prof. Victor Kopylov (GNIKHTEOS, Scientific-research State Institute of Chemistry and Technology of Organoelement Compounds; Moscow); α,ω-diepoxyoligo (dimethylsiloxane) (Scheme 1 b) and bis(hydroxyalkyl)polydimethylsiloxane ($M_n \approx 5.600$) (Scheme 1 d) were obtained from Aldrich Chemicals. Hexamethylenediamine was used as a hardener.

2.2. Sample preparation

Various amounts (3, 5, 10, 15 wt%) of the selected silicon-organic modifiers were directly mixed into the epoxy matrix. The components were stirred for 30–40 min at room temperature, then 7 wt% of the hexamethylenediamine hardener was added. Antibiocorrosive hybrid coatings were prepared by adding 1 or 3 wt% of transition metals (Co, Ni) coordination compounds of adamantane-containing hydrazide-hydrazones [24] and then 7 wt% of hexamethylenediamine into modified polymer matrices. The resulting light colored homogenous composites were kept for 48–72 h at room temperature. The compositional details of each hybrid material are presented in Table 1. The chemical structures of the coordination compounds are displayed in Scheme 2.

Table 1
Materials based on the ED-20 commercial epoxy.

#	Composite	#	Composite
1	pure ED-20	11	ED-20 / 15% EOMS
2	ED-20 / 5% SODCl	12	ED-20 / 3% BHODMS
3	ED-20 / 10% SODCl	13	ED-20 / 3% BHODMS / 1% CC
4	ED-20 / 10% SODCl / 1% CC	14	ED-20 / 3% BHODMS / 3% CC
5	ED-20 / 10% SODCl / 3% CC	15	ED-20 / 5% BHODMS
6	ED-20 / 15% SODCl	16	ED-20 / 5% BHODMS / 1% CC
7	ED-20 / 5% EOMS	17	ED-20 / 3% HMVOS
8	ED-20 / 10% EOMS	18	ED-20 / 3% HMVOS / 1% CC
9	ED-20 / 10% EOMS / 1% CC	19	ED-20 / 5% HMVOS
10	ED-20 / 10% EOMS / 3% CC	20	pure EOMS

2.3. Thermophysical characterization

The DSC measurements were performed with a differential scanning calorimeter from Netzsch, Selb, Germany, model DSC 200. All tests were conducted under dry nitrogen in the temperature range from −100 °C up to + 300 °C at a heating rate 5 °C/min. Samples of about 10 mg were enclosed in aluminium DSC capsules.

Thermogravimetric analysis (TGA) was carried out using an apparatus model Q1500D from MOM, Budapest, in the temperature range 30–700 °C and a heating rate 10 °C/min. Both DSC and TGA techniques are well explained by Menard [25].

a)

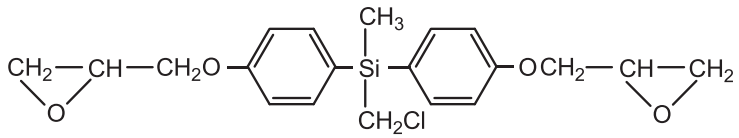

b)

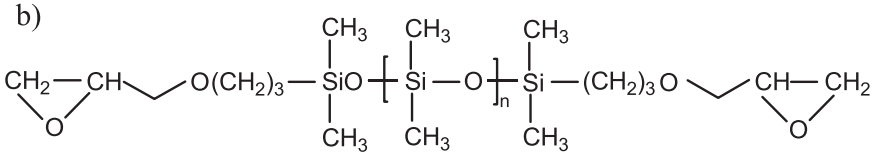

c)

$$HO\{[Si(CH_3)_2O]_{98.5}[Si(CH_3)(CH{=}CH_2)O]_{1.5}\}_xH, \text{ where } x = 3 \div 5$$

d)

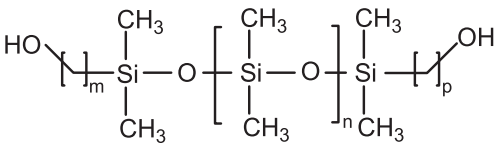

Scheme 1. a) Silicon-organic diepoxy with functional $-CH_2Cl$ groups at silicon atoms (SODCl). b) α,ω-Diepoxyoligo(dimethylsiloxane) (EOMS). c) α,ω-Dihydroxydimethyl(methylvinyl)oligoorganosiloxane (HMVOS). d) Bis(hydroxyalkyl)oligodimethylsiloxane (BHODMS).

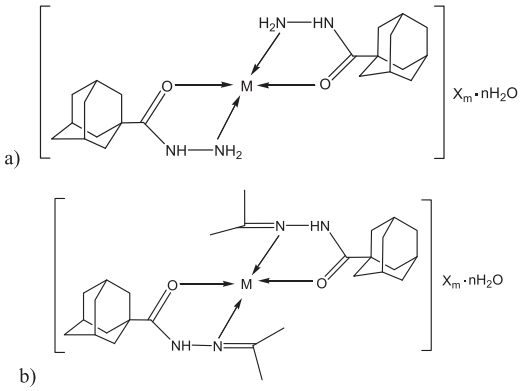

Scheme 2. Transition metals coordination compounds of adamantane-containing hydrazide-hydrazones. M = Co (a), 9.3 wt%; Ni (b), 8.3 wt%; X = CH_3COO^- (a, b); m = 2; n = 1 (a), 2 (b).

2.4. Tribological characterization

Scratch and sliding wear tests were performed by using a Micro-Scratch Tester (MST) from Anton Paar which applies a linearly increasing force in the range from 0.03 N to 30.0 N or else a constant force at room temperature. The technique has been explained in a review article [2]. The sliding wear (SWD) results were obtained by multiple scratching with a diamond tip along the same groove. Either in single scratching or in SWD, one obtains the penetration (instantanenous) depth R_p and the residual (healing) depth R_h determined two minutes later. Both R_p and R_h values were taken at the midpoint. The viscoelastic recovery φ is defined as:

$$\phi = \frac{R_p - R_h}{R_p} \times 100\% \quad (1)$$

The parameters for progressive scratch were: initial load 0.03 N, final load 30.0 N, loading rate 30.0 N/min, scanning load 0.03 N, scratch length 8.0 mm and scratch speed 5.9 mm/min. SDW were performed under a constant load of 5.0 N with the scratch length 5.0 mm. For each sample 10 scratch runs were performed, at the scratch velocity 10.0 mm/min at room temperature (25 ± 2 °C). The conical diamond intender with 200 μm of diameter and the cone angle of 120° was used.

Dynamic friction was measured using of a Nanovea pin-on-disk tribometer from Micro Photonics Inc. The friction is determined on the basis of the deflection of the elastic arm. Strain gauges bonded on the elastic body of the arm convert it in a force sensor and allow the direct measurement of the friction force. The rotation of the disk is driven by a servo-motor, between 0 rpm and 500 rpm. 440 steel balls made by Salem Specialty Balls with the diameter of 3.2 mm were used. The temperature was 20 ± 2 °C, the speed 100 rpm, the sliding distance 40 m, the radius 2.0 mm, the load 5.0 N, 3000 revolutions, the test durations 30 min.

The scanning electron microscope (SEM) from Nikon, the Eclipse ME 600 model, was used to observe the changes in the wear tracks after testing and study the possible modes of failure or deformation. Weight of the debris formed served as a measure of wear.

3. Synthesis

As already noted, our important aim is the evaluation of long-term antimicrobial activity of hybrid materials based on a commercial ED-20 epoxy resin. As modifiers we used silicon-organic compounds, containing functional groups at silicon atoms (Scheme 1).

The curing is exothermic; the resulting hardened resin has low elasticity. Earlier work suggested that silicon-organic oligomers might improve some properties of epoxy resins (elasticity, thermal stability, hydrophobicity etc.) acting as plasticizers [21]. Such oligomers could lower the heat release rate during the hardening of the epoxy and improve adhesion of the composites to various substrates. Scheme 1a displays an alternative route, without using the ED-20 epoxy. The resulting material used in small quantities could improve the strength, light stability and resistance against organic solvents [21].

As bioactive component for antibiocorrosive coatings we have used tricyclo[3.3.1.$1^{3,7}$]decane (adamantane) containing hydrazide-hydrazone coordination compounds (CCs) of certain transition metals (Co, Ni) (Scheme 2). The choice was dictated by their stability and the ability to form dipole-dipole and hydrogen bonds with the polymer matrix [24].

4. Thermophysical properties

We consider first DSC results. All materials studied are amorphous, melting transitions are not visible. Kalogeras and Hagg Lobland note that the glass transitions regions are usually broad [26]. Almost all our hybrids have glass transition regions beginning in the range between 49 °C and 58 °C.

DSC diagrams show also phase transitions in the glassy state, so called α-transitions. For brevity we do not include the diagrams here, only some numerical values pertaining to the transitions. Thus, going from composite 1 to 2 (for compositions return to Table 1), that is adding 3 wt% of BHODMS to ED-20, results in lowering the alpha transition temperature T_α centered around – 46 °C to one centered around – 62 °C. Apparently, the internal cohesion of pure epoxy at the low temperature is perturbed by the presence of siloxanes. On the other hand, composite 4 has T_α centered around 44 °C. Thus, addition of coordination compounds enhances the stability of the low temperature amorphous phase.

TGA results for neat epoxy and for some selected hybrids are displayed in Table 2. The non-modified epoxy matrix has the weight loss of 5.4% at 205 °C (Table 2). At 230 °C the weight loss is 8%. Intensive thermal degradation process of the pure epoxy matrix takes place in the range of 230–440 °C, the respective weight loss is 78%. The Table includes the temperature until which the hybrids are stable (T_{st}), so-called initial decomposition temperature (IDT; i.e. temperature, at which hybrids show first weight loss) and the temperature of maximum rate of degradation T_{max} (temperature after what no changes are observed).

As seen in Table 2, IDT and T_{max} of the modified epoxy hybrids increase with respect to the pure epoxy. Thus, resistance to thermal degradation is enhanced and weight loss is shifted to higher temperatures as the amount of modifier increases; these effects are enhanced further by addition of bioactive component.

Table 2
TGA data of the epoxy hybrids.

Hybrid	T_{st}, °C	T, °C	Weight loss, %	IDT, °C	T_{max}, °C
1	220	205	5.4	205	440
		230	8.0		
		440	78.0		
2	296	296	6.5	296	510
		510	76.9		
3	300	300	6.7	300	546
		546	71.3		
4	316	316	5.0	316	560
		560	81.5		
8	317	317	7.8	317	512
		512	77.9		
10	367	367	6.1	367	570
		570	75.9		
12	229	229	7.6	229	452
		452	78.6		
17	229	229	8.3	326	479
		452	74.2		
18	323	323	9.6	323	493
		493	65.1		

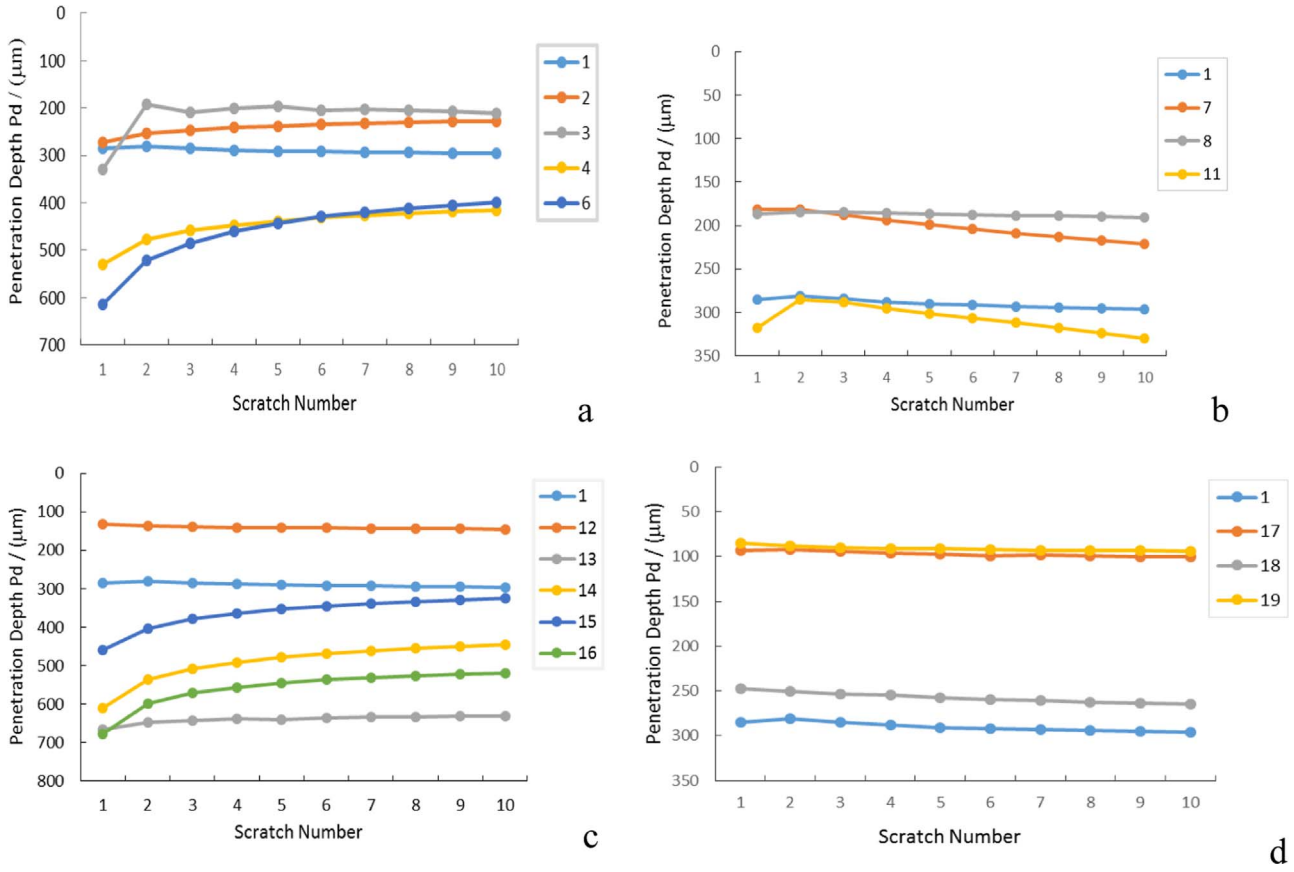

Fig. 1. Penetration depths of pure and modified hybrid composites: curve labeled 1 is for pure ED-20; a) 2 – 4 and 6 are for ED-20 modified with SODCl and CC; b) 7, 8 and 11 are for ED-20 modified with EOMS and CC; c) 12–16 are for ED-20 modified with BHODMS and CC; d) 17–19 are for ED-20 modified with HMVOS and CC.

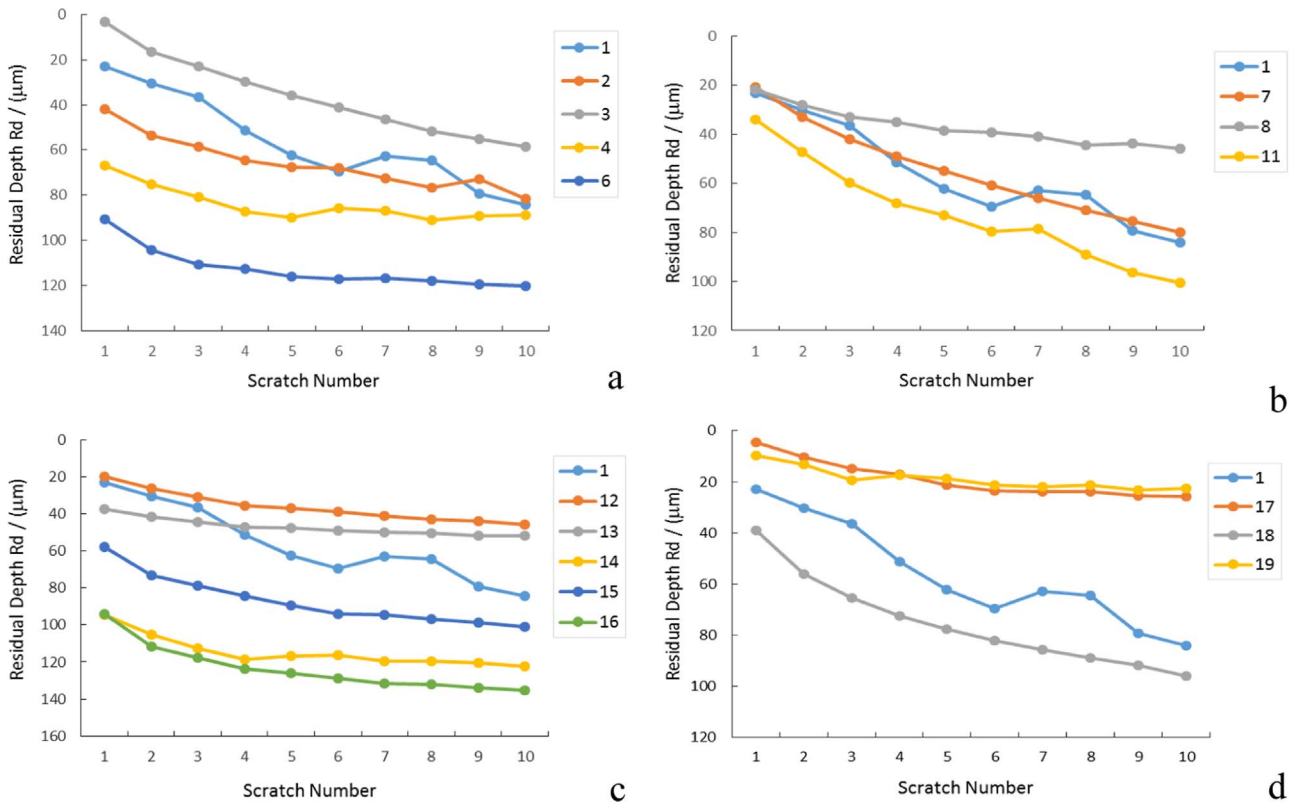

Fig. 2. Residual depths of pure and modified hybrid composites: curve 1 is for pure ED-20; a) 2–4 and 6 for ED-20 modified with SODCl and CC; b) 7, 8 and 11 for ED-20 modified with EOMS and CC; c) 12–16 for ED-20 modified with BHODMS and CC; d) 17–19 for ED-20 modified with HMVOS and CC.

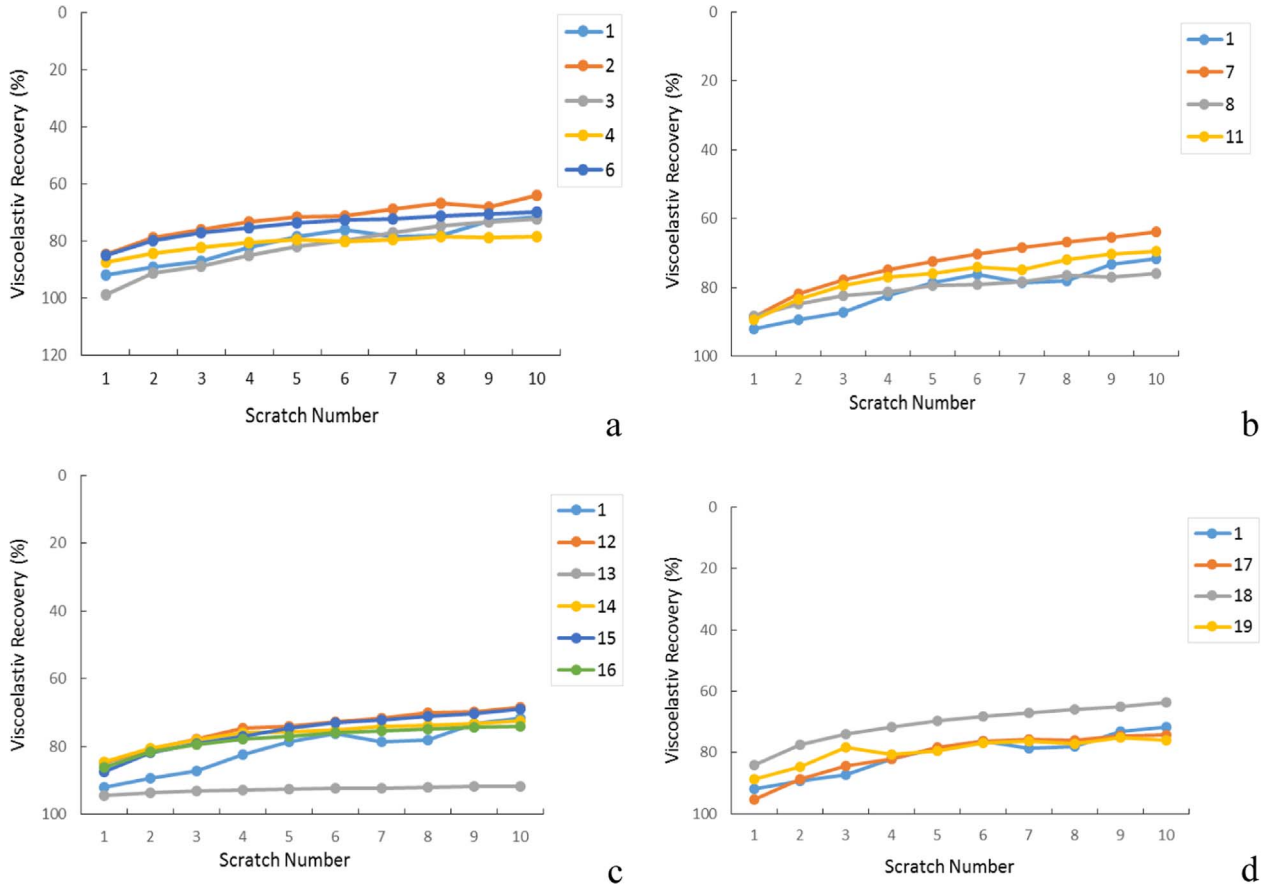

Fig. 3. Viscoelastic recovery of pure and modified hybrid composites: curve 1 for pure ED-20; a) 2–4 and 6 for ED-20 modified with SODCl and CC; b) 7, 8 and 11 for ED-20 modified with EOMS and CC; c) 12–16 for ED-20 modified with BHODMS and CC; d) 17–19 for ED-20 modified with HMVOS and CC.

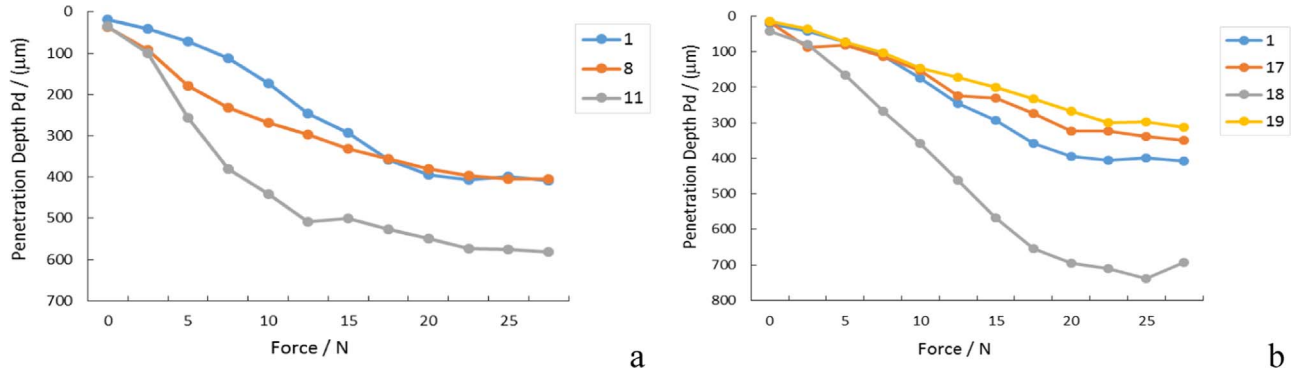

Fig. 4. Single scratch penetration depths as a function of the applied force: 1 for pure ED-20; a) 8 and 11 for ED-20 modified with EOMS and CC; b) 17–19 for ED-20 modified with HMVOS and CC.

5. Tribological properties

We begin with **sliding wear determination** (SWD) results obtained by multiple scratching along the same groove. We present the diagrams of the penetration and residual depths as a function of the run number at the constant force 5.0 N (Figs. 1 and 2, respectively). Numbers in the inserts pertain to the compositions defined in Table 1. Needless to say, the pure epoxy was examined as a reference.

As it is seen from curves of the penetration depth in Fig. 1, modification improves resistance of composites to instantaneous deformation by micro scratching. At the applied load, polymer composites 2 and 3 have the original penetration depth ranging from about 210–230 µm while pure epoxy has $R_p \approx 285$ µm. Further addition of modifier is counterproductive and displays higher values of penetration depth (Fig. 1; 6). Modification with 5 and 10 wt% of EOMS (Figs. 1; 7 and 8) provides also shallower R_p than the pure epoxy. Increasing modifier concentration slightly increases the penetration depth (Fig. 1; 11). Among the modifiers, silicon-organic oligomers show the largest reductions in R_p, the best result provided by HMVOS (Fig. 1; 17 and 19). In all cases, as it was expected, one observes an increase of penetration depth by incorporation of CCs in polymer matrices. These effects can be explained by the spatial structure of CCs, see again Scheme 2.

Fig. 2 shows the residual (after healing) depth R_h diagrams for our hybrid composites at a constant load as a function of the number of scratch test runs performed. Modifications with 5 and 10 wt% SODCl and EOMS and with silicon-organic oligomers largely cause decreases of the residual depth. After some initial increases of R_h with the increasing test number, most of our composites reach a constant residual depth;

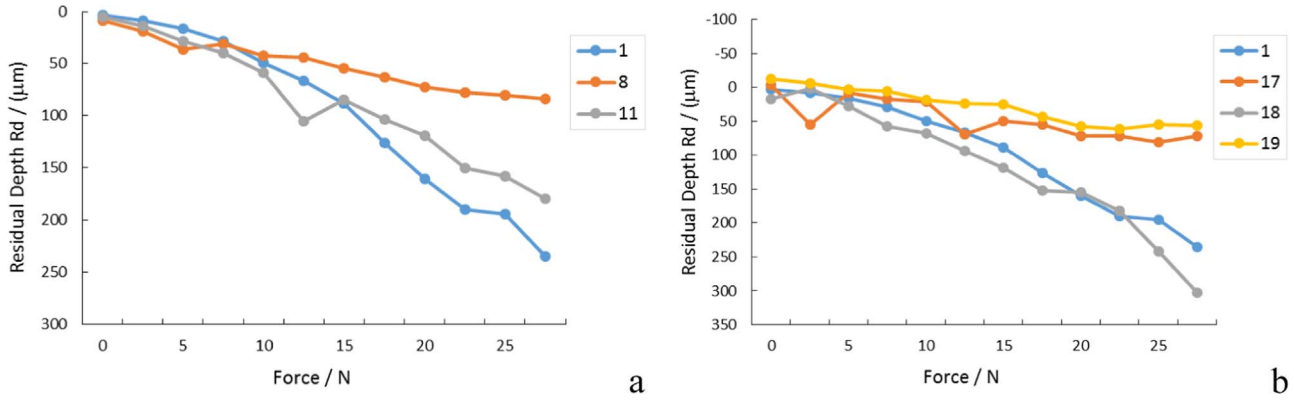

Fig. 5. Single scratch residual depths as a function of the applied force: 1 for pure ED-20; a) 8, 11 for ED-20 modified with EOMS and CC; b) 17–19 for ED-20 modified with HMVOS and CC.

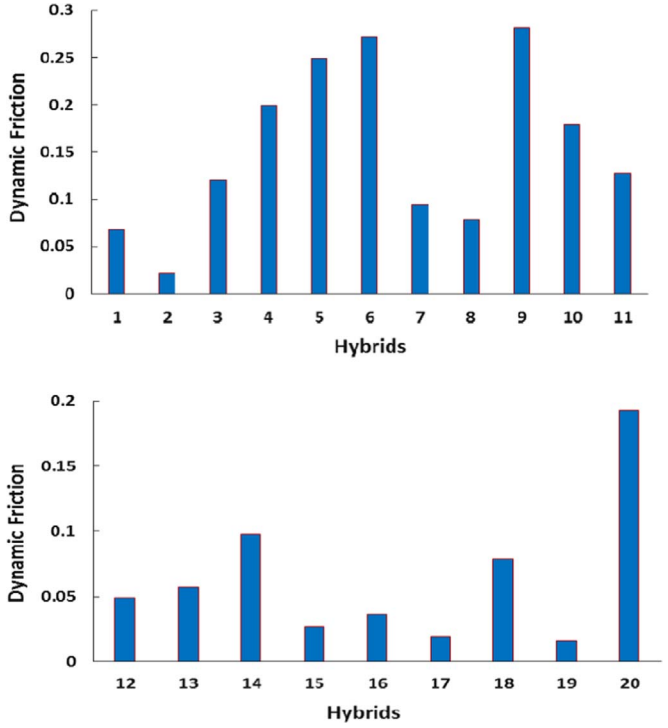

Fig. 6. Dynamic friction values after reaching a steady state.

further runs provide no change. The phenomenon of strain hardening in SWD was first reported in 2004 [27]. It was the starting point for the equation defining brittleness B and relating it to φ; for other relations between B and other properties see [28].

As for the viscoelastic recovery, the values of φ calculated from Eq. (1) are in the range between 64% and 95%. A very good result (92–95%) is seen for the composite modified with 3 wt% BHODMS (Table 1; Fig. 3, curve 13).

Single scratching results: progressive scratch testing for selected composites are shown in Fig. 4 as R_p vs. force N diagrams. We see stronger resistance to the instantaneous penetration for composites 17 and 19.

Fig. 5 shows selected residual depth R_h vs. the applied force diagrams. The samples modified with 10 wt% EOMS and with 3 and 5 wt% HMVOS have the shallowest R_h in comparison with pure epoxy, results in agreement also with those shown for the penetration depth in Fig. 4. Thus modification can improve scratch resistance – in function of the modifier type and its quantity.

5.1. Friction results

Dynamic friction (f) was monitored with the aid of a linear variable displacement transducer and was continuously recorded throughout the tests. After 40 m distance, dynamic friction for all tested materials varied in the range $0.01 < f < 0.25$. For pure epoxy, the friction increases in the initial stage of sliding before reaching a steady stage. The modification with silicon-organic oligomers BHODMS/HMVOS provides the largest reduction of dynamic friction with respect to the pure epoxy. This behavior is related to already mentioned plasticizing ability of flexible siloxane oligomers.

The dynamic friction results are summarized in Fig. 6.

We see in Fig. 6 that addition of 5 wt% SODCl (hybrid # 2) provides the lowest friction value of all. This might be explained by formation of "bumps" causing a decrease of the effective surface area of the hybrid with respect to the steel balls. However, adding 10% (hybrid # 3) or 15% (# 6) of SODCl causes large increases in friction; apparently the bumps increase their surfaces.

Interesting also are hybrids 17 and 19 containing HMVOS, with dynamic friction values also much lower than neat epoxy. We recall that these materials also show low depth values in scratch testing; see again Figs. 1d, 2d, 4b and 5b. It is expected that low depth values in one time scratching are also reflected in sliding wear determination. However, low friction values by no means automatically mean low wear and high scratch resistance [29]. In fact, for phenolic resin + carbon fibers composites with carbon nanotubes (CNTs) added, weight loss decreases with increasing concentration of CNTs; dynamic friction increases at the same time [30]. We also need to cite the statement of Hutchings and Shipway that both load and sliding speed affect friction substantially [31]. This is the case for instance of composite bearings on steel that are based on polytetrafluoroethylene (PTFE) [31].

6. Scanning electron microscopy observations

Our SEM observation of surface microstructures after tribological tests seems to support our interpretation of the tribology results. Selected results are displayed in Fig. 7. A non-modified epoxy shows significant amounts of wear debris and crack formation. The wear tracks in the cases of modified epoxy hybrids are much less pronouced and show a more ductile behavior (Fig. 7; 8, 11–17). Interestingly, a worn track surface for composite 13 exhibits layer-like waves what can be explained by incorporation of spatial structure of CC (Scheme 2).

7. Water absorption and aging

We have performed aging at 40 °C and 60 °C in the air to determine weatherability (complex action of moisture, air oxygen, carbon dioxide and visible light) of our hybrids. For six months all samples maintained

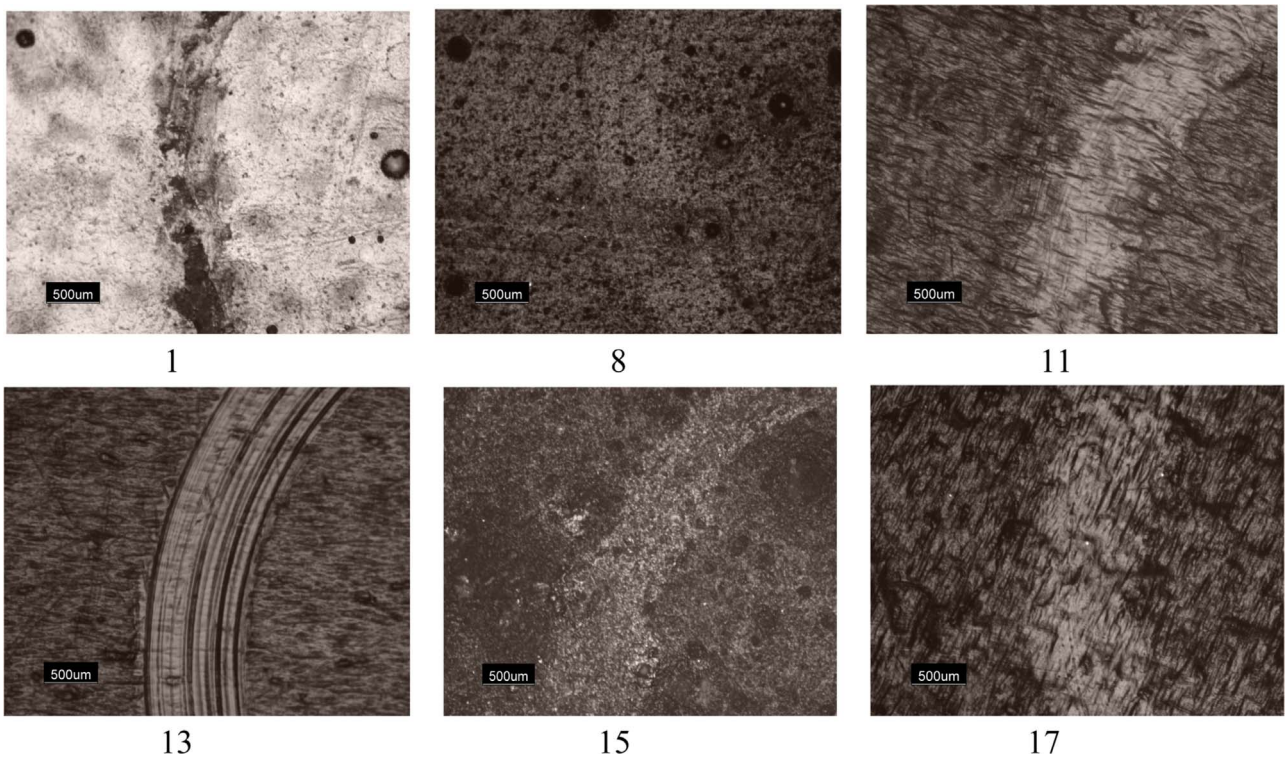

Fig. 7. SEM micrographs of epoxy based hybrid materials after testing.

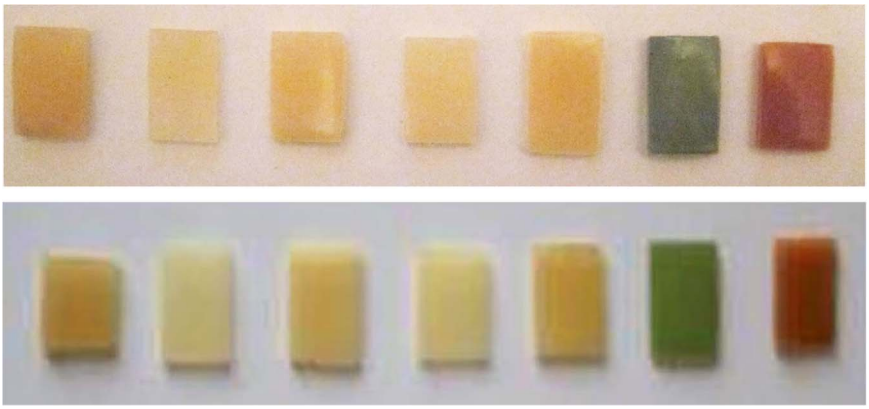

Fig. 8. Images of some hybrid materials (from left to right: 3, 11, 15, 17, 6, 4 and 16; Table 1) originally (top) and after 6 months (bottom).

their initial appearance, color, optical transparency and mechanical properties (surface homogeneity without splits formation); see Fig. 8.

Moisture medium affects the rate of microbial attachment and microbe dissemination on various materials [32]. Thus, hydrophobic properties of coatings play significant role in the process of adhesion of microorganisms on various surfaces. We have determined water absorption ability (W_{H2O}, wt%) of our antibiocorrosive coatings by gravimetry [24]. As Fig. 9 shows, W_{H2O} during 720 h does not exceed 0.01 wt% in all cases. Thus, the dry experimental condition in our tests is close to the real application conditions of our hydrophobic hybrids.

8. Concluding remarks

Our modifications of the basic epoxy results in some cases in significant improvement of scratch resistance, lowering of dynamic friction and also lower water absorption. Thus, modification with 5 and 10 wt% EOMS provides shallower penetration depths than that of the pure epoxy. Increasing modifier concentration slightly increases the R_p. Among the modifiers, silicon-organic oligomers show the largest reductions in R_p, the best result provided by HMVOS. The samples modified with 10 wt% EOMS and with 3 and 5 wt% HMVOS have the shallowest R_h in comparison with pure epoxy. The values of viscoelastic recovery are in the range between 64% and 95%. A very good result (92–95%) is seen for the composite modified with 3 wt% BHODMS.

Dynamic friction for all tested materials varies in the range 0.01–0.25. The modification with 5 wt% SODCl and silicon-organic oligomers BHODMS/HMVOS provides the largest reduction of dynamic friction with respect to the pure epoxy. The bioactive components cause a slight increase of dynamic friction, but still the resulting values are lower than for the unmodified neat epoxy. Such modifications are actually easier to implement than improvement of tribology of surfaces by burnishing and nitriding [33].

Characterization of composites by DSC show that almost all hybrids have glass transition regions in the range of 49–58 °C. Addition of coordination compounds enhances the stability of the low temperature amorphous phase. Enhanced resistance to thermal degradation of modified epoxy hybrids with respect to the pure epoxy is shown by TGA results; IDT is shifted from 220 °C to 296–367 °C and T_{max} is shifted from 440 °C to 480–570 °C. As noted above, the water absorption ability (W_{H2O}) of our hybrids during 720 h does not exceed 0.01 wt% in

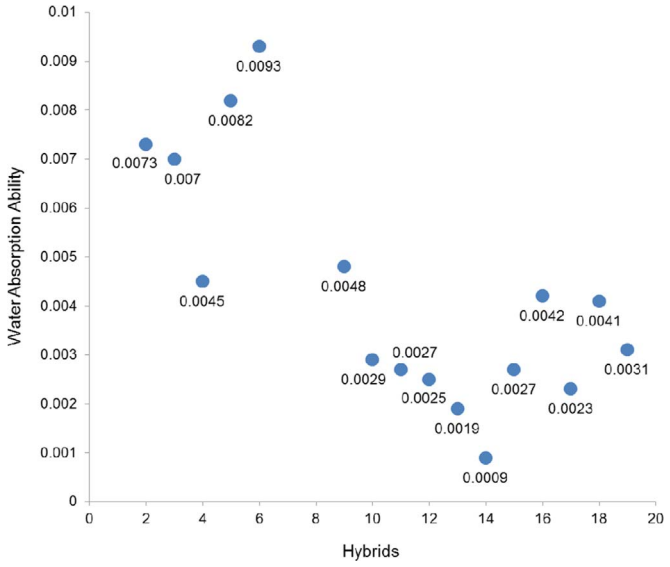

Fig. 9. Water absorption of our hybrids after 720 h.

all cases. SEM micrographs of surfaces of our hybrids confirm that their wear resistance increased compared to the non-modified epoxy.

Potential applications areas of our hybrids include antibiocorrosive protection of cultural heritage and museum exhibits.

The basic tenet of Materials Science and Engineering tells us that macroscopic properties are determined by structures and interactions at the atomic and molecular level. On this basis, there is a quest for establishing connections between different macroscopic properties [34]. However, as Peter Blau warns us [29], even a single property can result from a number of factors: “The friction coefficient is an established, but somewhat misunderstood, quantity in the field of science and engineering. It is a convenient and useful parameter for engineering, but care should be exercised when ascribing to it a fundamental significance. For hundreds of years, friction coefficients have served many useful purposes, like aiding in the design of machines and buildings, improving devices for enhanced safety (like brakes, floor waxes, tires, and walkways), and improving industrial processes. While friction coefficients are relatively easy to determine in laboratory experiments, the fundamental origins of sliding resistance are not as clear. In fact, some of the greatest scientists and philosophers have contemplated friction without managing to produce a universal, predictive theory. This striking lack of success is due to the many potential factors that can influence friction in a wide spectrum of physical situations”.

Acknowledgments

Authors would like to thank the Shota Rustaveli National Science Foundation (RNSF) of Georgia, Tbilisi, for financial support and also Prof. Victor Kopylov, GNIKHTEOS (Scientific-research State Institute of Chemistry and Technology of Organoelement Compounds Compounds, Moscow) for synthesis and providing us the silicon-organic diepoxy oligomer and α,ω-dihydroxydimethyl(methylvinyl)oligoorganosiloxane.

References

[1] I.M. Hutchings, Leonardo da Vinci’s Studies of friction, Wear 360 (2016) 51–66.
[2] J. Khedkar, I. Negulescu, E.I. Meletis, Sliding wear behavior of PTFE composites, Wear 252 (2002) 361–369.
[3] W. Brostow, V. Kovacevic, D. Vrsaljko, J. Whitworth, Tribology of polymers and polymer-based composites, J. Mater. Educ. 32 (2010) 273–290.
[4] Y. Yamamoto, T. Takashima, Friction and wear of water lubricated PEEK and PPS sliding contacts, Wear 253 (2002) 820–826.
[5] N. Espallargas, C. Torres, A.I. Muñoz, A metal ion release study of CoCrMo exposed to corrosion and tribocorrosion conditions in simulated body fluids, Wear 332–333 (2015) 669–678.
[6] H.A. Videla, Prevention and control of biocorrosion, Int. Biodeterior. Biodegrad. 49 (2002) 259–270.
[7] J.-D. Gu, Microbiological deterioration and degradation of synthetic polymeric materials: recent research advances, Int. Biodeterior. Biodegrad. 52 (2003) 69–91.
[8] European Commission, Preserving our heritage, improving our environment, (2009), p. 248.
[9] International Standard ISO 846:1997 (E), Plastics – Evaluation of the Action Of Microorganisms, 2nd Ed., (1997), p. 22.
[10] R. Gómez-Romero, C. Sanchez, Hybrid materials, functional applications: an introduction, in: P. Gómez-Romero, C. Sanchez (Eds.), Functional Hybrid Materials, Wiley-VCH, Weinheim/Bergstrasse, 2004, pp. 1–14.
[11] Yu. V. Savelyev, E.R. Akhranovich, A.P. Grekov, V.V. Korskanov, V.I. Shtompel, V.P. Privalko, P. Pissis, A. Kanapitsas, Influence of chain extenders and chain end groups on properties of segmented polyurethanes. I. phase morphology, Polymer 39 (1998) 3425–3429.
[12] G.H. Michler, F.J. Balta-Calleja, Nano- and Micromechanics of Polymers: Structure Modification and Improvement of Properties, Hanser, Munich–Cincinnati, 2012.
[13] G.H. Michler, Atlas of Polymer Structures, Hanser, Munich–Cincinnati, 2016.
[14] R.C. Desai, R. Kapral, Dynamics of Self-organized and Self-assembled structures, Cambridge University Press, Cambridge–New York, 2009.
[15] F. Baino, E. Verné, C. Vitale-Brovarone, Feasibility, tailoring and properties of polyurethane/ bioactive glass composite scaffolds for tissue engineering, J. Mater. Sci. Med. 20 (2009) 2189–2195.
[16] C.A. May, Introduction to epoxy resins, in: C.A. May (Ed.), Epoxy Resins Chemistry and Technology, Marcel Dekker, New York, 1988, pp. 1–8.
[17] B. Bilyeu, W. Brostow, K.P. Menard, Epoxy thermosets and their applications II. Thermal analysis, J. Mater. Educ. 22 (2000) 107.
[18] Y. Yarovsky, E. Evans, Computer simulation of structure and properties of cross-linked polymers: application to epoxy resins, Polymer 43 (2002) 963–969.
[19] L. Rey, N. Poisson, A. Maazouz, H. Sauterau, Enhancement of crack propagation resistance in epoxy resins by introducing poly(dimethylsiloxane) particles, J. Mater. Sci. 34 (1999) 1775–1781.
[20] L. Könczöl, W. Döll, U. Buchholz, R. Mülhaupt, Ultimate properties of epoxy resins modified with a polysiloxane–polycaprolactone block copolymer, J. Appl. Polym. Sci. 26 (1995) 371–377.
[21] D. Murachishvili, E. Markarashvili, Sh. Samakashvili, N. Chedia, N. Lekishvili, N. Tsomaia, Protective coatings based on silicon-organic epoxide and methacrylic copoymers, Proceedings Acad. Sci. Georgia, Chem. 30 235-240, 2004.
[22] N. Lekishvili, S.H. Samakashvili, G. Lekishvili, Z. Pachulia, New carbofunctional oligosiloxanes for the substrates of antibiocorrosive covers, Polym. Res. J. 3 (2009) 225–238.
[23] N. Lekishvili, Kh. Barbakadze, Synthesis and characterization of transition metals coordination compounds of bioactive spatial alicyclic hydrazide-hydrazones, Asian J. Chem. 24 (2012) 2637–2642.
[24] T.A. Travinskaia, E.A. Mishuk, L.N. Perepelitisina, Yu.V. Savyelyev, Obtaining and properties of biodegradable materials based on ionomer polyurethane and polysaccharide, Polim. Zh. 32 (2010) 66–74.
[25] K.P. Menard, Ch. 6 in Performance of Plastics, W. Brostow (Ed.), Hanser, Munich - Cincinnati 2000.
[26] I.M. Kalogeras, H.E. Hagg Lobland, The nature of the glassy state: structure and transitions, J. Mater. Educ. 34 (2012) 69–94.
[27] W. Brostow, G. Damarla, J. Howe, D. Pietkiewicz, Determination of wear of surfaces by scratch testing, e-Polymers 025 (2004) 1–6.
[28] W. Brostow, H.E. Hagg Lobland, S. Khoja, Brittleness and toughness of polymers and other materials, Mater. Lett. 159 (2015) 478–480.
[29] P.J. Blau, The significance and use of the friction coefficient, Tribol. Int. 34 (2001) 585–591.
[30] D.-S. Lim, J.-W. An, H.J. Lee, Effect of carbon nanotube addition on the tribological behavior of carbon/carbon composites, Wear 252 (2002) 512–517.
[31] I. Hutchings, P. Shipway, Tribology: Friction and Wear of Engineering Materials, Section 9.2, Butterworth-Heinemann, Oxford, 2017.
[32] R.M. Donlan, Biofilms: microbial life on surfaces, Emerg. Infect. Dis. 8 (2002) 881–890.
[33] L. Janczewski, D. Tobola, W. Brostow, K. Czechowski, H.E. Hagg Lobland, M. Kot, K. Zagorski, Effects of ball burnishing on surface properties of low density polyethylene, Tribol. Int. 93 (2016) 36–42.
[34] W. Brostow, H.E. Hagg Lobland, Materials: Introduction and Applications, John Wiley & Sons, New York, 2017.